Delft University of Technology

On the origin of amplitude reduction mechanism in tapping mode atomic force microscopy

Keyvani Janbahan, Sasan; Sadeghian, Hamed; Goosen, Hans; Van Keulen, Fred

DOI
10.1063/1.5016306

Publication date
2018

Document Version
Final published version

Published in
Applied Physics Letters

Citation (APA)
Keyvani Janbahan, S., Sadeghian, H., Goosen, H., & Van Keulen, F. (2018). On the origin of amplitude reduction mechanism in tapping mode atomic force microscopy. *Applied Physics Letters*, *112*(16), Article 163104. https://doi.org/10.1063/1.5016306

Important note
To cite this publication, please use the final published version (if applicable).
Please check the document version above.

Copyright
Other than for strictly personal use, it is not permitted to download, forward or distribute the text or part of it, without the consent of the author(s) and/or copyright holder(s), unless the work is under an open content license such as Creative Commons.

Takedown policy
Please contact us and provide details if you believe this document breaches copyrights.
We will remove access to the work immediately and investigate your claim.

This work is downloaded from Delft University of Technology.
For technical reasons the number of authors shown on this cover page is limited to a maximum of 10.

On the origin of amplitude reduction mechanism in tapping mode atomic force microscopy

Aliasghar Keyvani, Hamed Sadeghian, Hans Goosen, and Fred van Keulen

Citation: Appl. Phys. Lett. **112**, 163104 (2018); doi: 10.1063/1.5016306
View online: https://doi.org/10.1063/1.5016306
View Table of Contents: http://aip.scitation.org/toc/apl/112/16
Published by the American Institute of Physics

Articles you may be interested in

Chaos: The speed limiting phenomenon in dynamic atomic force microscopy
Journal of Applied Physics **122**, 224306 (2017); 10.1063/1.5000130

Invisible magnetic sensors
Applied Physics Letters **112**, 162406 (2018); 10.1063/1.5023565

Significant improvement in the electrical characteristics of Schottky barrier diodes on molecularly modified Gallium Nitride surfaces
Applied Physics Letters **112**, 163502 (2018); 10.1063/1.5005587

Noise assisted pattern fabrication
Applied Physics Letters **112**, 161601 (2018); 10.1063/1.5021529

Growth of boron-doped few-layer graphene by molecular beam epitaxy
Applied Physics Letters **112**, 163103 (2018); 10.1063/1.5019352

Mid-infrared GaSb-based resonant tunneling diode photodetectors for gas sensing applications
Applied Physics Letters **112**, 161107 (2018); 10.1063/1.5025531

PHYSICS TODAY
WHITEPAPERS

MANAGER'S GUIDE

Accelerate R&D with
Multiphysics Simulation

READ NOW

PRESENTED BY

APPLIED PHYSICS LETTERS **112**, 163104 (2018)

On the origin of amplitude reduction mechanism in tapping mode atomic force microscopy

Aliasghar Keyvani,[1,2] Hamed Sadeghian,[2,3,a)] Hans Goosen,[1] and Fred van Keulen[1]
[1]*Department of Precision and Microsystems Engineering, Faculty of Mechanical, Maritime and Materials Engineering, Delft University of Technology, 2628 CD Delft, The Netherlands*
[2]*Netherlands Organization for Applied Scientific Research, TNO, 2628 CK Delft, The Netherlands*
[3]*Department of Mechanical Engineering, Eindhoven University of Technology, 5600MB Eindhoven, The Netherlands*

(Received 17 November 2017; accepted 11 March 2018; published online 20 April 2018)

The origin of amplitude reduction in Tapping Mode Atomic Force Microscopy (TM-AFM) is typically attributed to the shift in resonance frequency of the cantilever due to the nonlinear tip-sample interactions. In this paper, we present a different insight into the same problem which, besides explaining the amplitude reduction mechanism, provides a simple reasoning for the relationship between tip-sample interactions and operation parameters (amplitude and frequency). The proposed formulation, which attributes the amplitude reduction to an interference between the tip-sample and dither force, only deals with the linear part of the system; however, it fully agrees with experimental results and numerical solutions of the full nonlinear model of TM-AFM. *Published by AIP Publishing.* https://doi.org/10.1063/1.5016306

The origin of the amplitude mechanism in Tapping Mode Atomic Force Microscopy (TM-AFM) was a fundamental research question in the late 1990s and was already answered at that time.[1] Briefly, *The amplitude reduces because the resonance frequency of the cantilever-surface system changes*. Moreover, the energy dissipation between the tip and the sample during the contact contributes to the amplitude reduction. This explanation is graphically demonstrated in Fig. 1, and more details can be found in Ref. 2. Although many aspects of TM-AFM are well described by this explanation, several recent observations on Tip Sample Interaction (TSI) force are not very easy to explain, in particular, the relationship between the TSI force and the operation parameters (excitation frequency and set-point amplitude). In this letter, we present a different description for the origin of amplitude reduction in AFM that also rigorously explains the recent observations.

It must be acknowledged that the traditional explanation based on the resonance frequency shift is mathematically precise and is based on a nonlinear dynamics study of the cantilever in the presence of the Derjaguin-Muller-Toporov (DMT) force model.[3] The only two simplifications which have been used in the formulations of the existing theory are (i) the cantilever is modeled as a one degree of freedom (DOF) resonator and (ii) the motion of the cantilever is assumed harmonic, even in the presence of strongly nonlinear TSI. There are exceptional cases for which the motion of the cantilever is not harmonic, and hence, the aforementioned assumptions are not valid anymore (such as multi-frequency AFM, transient situations, and aqua medium measurements[4–7]). Yet, experiments and numerical simulations confirm that for the single harmonic TM-AFM in air, none of these assumptions are restricting, and the existing theory, i.e., based on the frequency shift, is precise.[8] However, with this theory, the relationship between the operation parameters and the TSI force is not easily explained. For example, the maximum interaction force during each cycle, i.e., the Peak Repulsive Force (PRF), is commonly considered to be a function of the amplitude and stiffness of the cantilever.[9–11] Nonetheless, recent observations show that the excitation frequency is predominantly more important than the amplitude.[12] Without considering the excitation frequency, Xue *et al.*[10] reported a contradiction between their experimental results and the ones presented by Su *et al.*,[11] which is not explained with the existing theory. Xue *et al.*[10] observed a descending trend between the amplitude ratio and the tip wear, whereas they expected an ascending relationship based on the previous TSI force measurements reported by Su *et al.*[11] In fact, depending on the excitation frequency, both could be valid. If the excitation frequency is chosen slightly lower than the resonance frequency of the

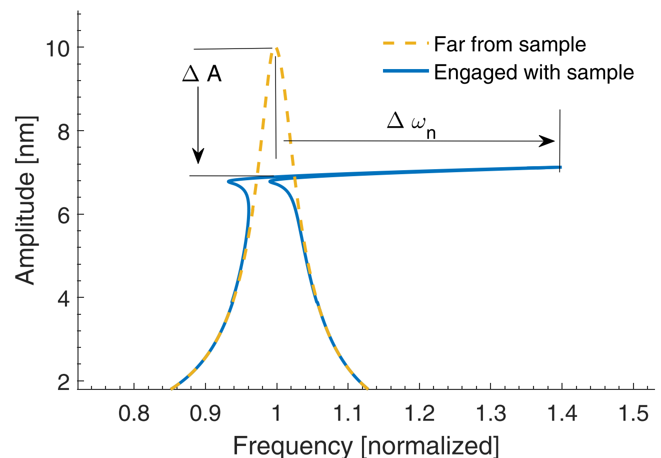

FIG. 1. Graphical explanation of amplitude reduction based on the resonance frequency shift. Since the nonlinear resonance frequency of the cantilever shifts ($\Delta\omega_n$), the amplitude reduces (ΔA). The details of the model used for this graph can be found in the supplementary material.

a)Electronic mail: hamed.sadeghianmarnani@tno.nl

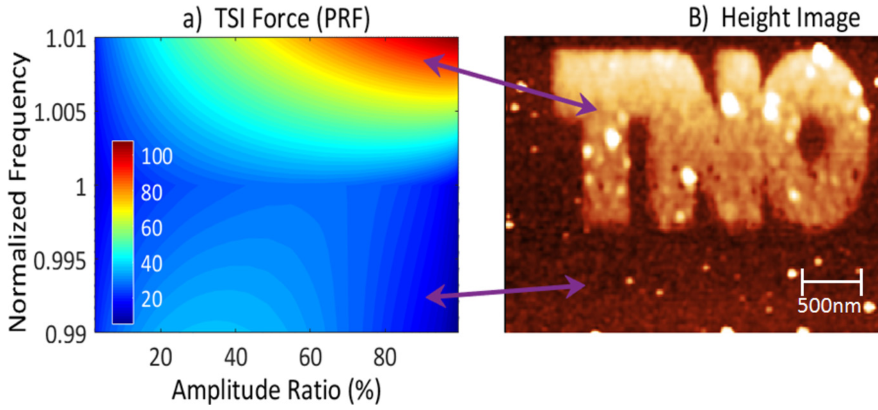

FIG. 2. (a) Peak Repulsive Force (PRF) versus amplitude ratio and normalized excitation frequency. The PRF is normalized with respect to the free air amplitude multiplied by the spring constant of the cantilever. The details of the mathematical model for this can be found in the supplementary material. (b) An example of nanopatterning using TM-AFM by tuning the TSI force via changing the excitation frequency. Reprinted with permission from Keyvani *et al.*, Proc. SPIE **9778**, 977818 (2016). Copyright 2016 Wiley-VCH Verlag GmbH & Co. KGaA.[12]

cantilever, the trend of the TSI force resembles the ones reported in Ref. 11, and if higher, the trend resembles Ref. 10.

To demonstrate the effect of excitation frequency, Fig. 2(a) shows the PRF versus both the amplitude ratio and the excitation frequency. The PRF is calculated using the fully nonlinear multi-DOF model of the cantilever. As it can be seen, the PRF has a saddle-shape trend with respect to the amplitude ratio and the excitation frequency. Thus, the amplitude-force relationship can be ascending or descending. Using these trends, we have previously demonstrated an AFM-based nano-patterning technique, Fig. 2(b), in which the TSI force was controlled via the excitation frequency, without changing the amplitude or the excitation power.[12] Without changing the excitation power and the set-point amplitude, the desired patterns could be transferred to the surface, without interrupting the imaging process. However, it was not possible to explain the results in Fig. 2 with the shift in resonance frequency. Therefore, this letter presents another perspective for the origin of amplitude reduction in TM-AFM, which also explains the frequency dependency of the TSI force.

Consider the cantilever as a linear 1-DOF resonator which is excited by a dithering force and nonlinearly interacts with the surface through the TSI force. The normalized governing differential equation for this 1-DOF model is

$$\ddot{x} + \xi\dot{x} + x = f_d \Re(e^{j\omega t}) + f_{ts}(x, \ldots), \tag{1}$$

where x, ξ, ω, f_d, and $f_{ts} \in \mathbb{R}$ represent the normalized tip-displacement, the damping coefficient, the normalized excitation frequency, the nondimensional dither force, and the TSI force, respectively. A dot represents the time derivation, $\Re$ is the real operator, and $j^2 = -1$.

The TSI force depends nonlinearly on the tip displacement and other physical and geometric parameters. Nonetheless, without any loss of generality, it can be considered as an unknown signal in the time domain.

Figure 3 graphically explains this idea. Although there exists a relationship between the TSI force and the displacement of the cantilever, in this letter, we set the system boundaries around *the cantilever* and keep the TSI force as an unknown input which can have any nonlinear relationship with the displacement of the cantilever. By keeping the TSI force unknown during the derivation of the model, we aim to present a formulation which explains the amplitude reduction mechanism in TM-AFM, *independent* of the interaction models. Moreover, since all the nonlinearity is hidden in the TSI force, we may benefit from the linear dynamics of the cantilever itself.

In steady state conditions, both the displacement and the TSI force are periodic in time. Hence, they both have a Fourier decomposition, with a first component at the same frequency as the excitation signal. The Fourier decomposition of the (unknown) TSI force and the tip displacement can be written as

$$f_{ts}(t) = \sum_{n=0}^{\infty} \Re(F_{ts}^{(n)} e^{nj\omega t}), \tag{2a}$$

$$x(t) = \sum_{n=0}^{\infty} \Re(X^{(n)} e^{nj\omega t}), \tag{2b}$$

where $F_{ts}^{(n)} = |F_{ts}^{(n)}| e^{-j\varphi_{ts}^{(n)}} \in \mathbb{C}$ is the n-th Fourier coefficient of the TSI force ($n \in \mathbb{N}$). $F_{ts}^{(n)}$ contains both the amplitude $[|F_{ts}^{(n)}|]$ and the phase $[\varphi_{ts}^{(n)}]$ of the TSI force. In the same manner, $X^{(n)} = |X^{(n)}| e^{-j\varphi_x^{(n)}} \in \mathbb{C}$ represents the amplitude ($|X|^{(n)}$) and the phase ($\varphi_x^{(n)}$) of the nth Fourier component (i.e., harmonic) of the motion of the cantilever. Considering Eq. (2), the system represented by Eq. (1) has an analytical solution for each of its frequency components as

$$X^{(n)} = \frac{e^{-j\arctan\left(\frac{n\xi\omega}{1-n^2\omega^2}\right)}}{\sqrt{(1-n^2\omega^2)^2 + n^2\xi^2\omega^2}} F_{tot}^{(n)}, \tag{3}$$

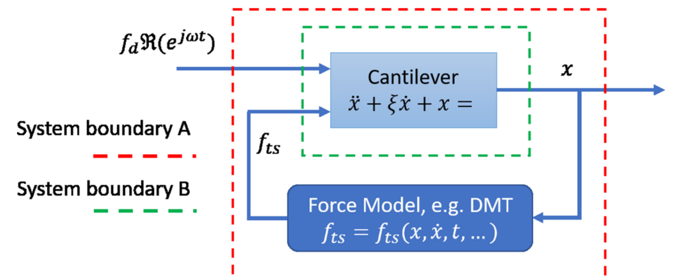

FIG. 3. Schematic representation of Eq. (1). The red (a) and green (b) dashed lines represent the system boundaries used in previous theories and the present model, respectively. The proposed model keeps the nonlinear relationship between the TSI force and the displacement out of the boundaries of the system, by assuming the TSI force to be an unknown input.

where $F_{tot}^{(n)} \in \mathbb{C}$ represents the n-th Fourier component of the total force acting on the cantilever. Note that $F_{tot}^{(1)} = f_d + F_{ts}^{(1)}$ and $F_{tot}^{(n)} = F_{ts}^{(n)}$, $n = 2, 3, \ldots$.

In conventional TM-AFM configurations, only the amplitude and the phase of the first harmonic motion [$X^{(1)}$] can be reliably measured and used in the control loop. Hence, in the rest of this letter, we only consider the first Fourier component of the force and displacement. Note that due to the (i) linearity of Eq. (1) and (ii) the orthogonality of the harmonic functions, the higher frequency content of the force does not have any effect on the first Fourier component of the motion.

Figure 4 (Multimedia view) depicts a normalized version of Eq. (3) as a phasor plot, in which the first Fourier coefficient of the forces and displacement [$F_d, F_{ts}^{(1)}, X^{(1)}$] are represented. All the phase values are measured with respect to the dither signal, and amplitudes are normalized. In this case, the cantilever is excited exactly at its resonance frequency ($\omega = 1$). Initially, i.e., in the absence of the TSI force (far from the sample), the displacement has a normalized amplitude equal to one and a phase delay of 90° (dashed green).

By bringing the cantilever closer to the sample, the tip starts to interact with the sample and the TSI force depends on the displacement. As mentioned earlier, the total harmonic force at the frequency of interest [$F_{tot}^{(1)}$, solid blue in Fig. 4] is the summation of the TSI force and the dither force, which generates the displacement [$X^{(1)}$, dashed blue]. Due to the linearity of the 1-DOF model, the amplitude of the displacement scales linearly with the amplitude of the total force, and its phase is 90° behind the total force.

Assuming that the contact between the tip and the sample is conservative [$F_{ts} = F_{ts}(x(t))$], the first Fourier component of the TSI force [$|F_{ts}^{(1)}|$] can be either 0° or 180° out of phase with respect to the displacement $X^{(1)}$. In the repulsive regime—which is the case for the majority of experiments (Also Fig. 4)—this phase delay is 180°, whereas for the attractive regime, it is 0. As shown in Fig. 4, since the TSI force (purple) is more than 90° out of phase with the dither force (solid green), the amplitude of total force [$|F_{tot}^{(1)}|$, solid blue] is less than the amplitude of the dither force alone [$|F_{tot}^{(1)}| = |F_{ts}^{(1)} + f_d| < f_d$]. Consequently, the amplitude of the motion in the engaged situation (dashed blue) is less than the free air amplitude (dashed green).

In short, the following causality loop governs the TM-AFM: (i) the phase of the TSI force depends on the displacement via the force-distance relationship (180° in Fig. 4), (ii) the phase of the displacement depends on the total force via the linear dynamics of the cantilever (90° in Fig. 4), and (iii) the total force is the summation of the dither force and the TSI force. Since the TSI force is out of phase with respect to the dither force, the amplitude of the total harmonic force is less than the dither force. Consequently, the engaged amplitude is less than the free air amplitude.

Translating the Fourier coefficients back to the harmonic functions, the origin of the amplitude reduction in TM-AFM can be explained as a destructive interference, i.e., partial cancellation, of the dither force and the first Fourier component of TSI force. The other Fourier components of the TSI force may or may not induce a motion at their own frequencies but certainly do not contribute to the amplitude or the phase at the frequency of interest at which the cantilever is driven and measured.

To generalize the above explanation for arbitrary excitation frequencies and non-conservative forces, we rewrite Eq. (3) with and without the TSI force. Considering the amplitude ratio (A_r) which is also the ratio between the amplitude of the total forces [$|f_d + F_{ts}^{(1)}| = A_r f_d$], the first Fourier component of the TSI force [$|F_{ts}^{(1)}|, \varphi_{ts}^{(1)}$] can be calculated from

$$A_r f_d e^{j\left(\varphi_{ts}^{(1)} - \theta_X^{ts} - \arctan\left(\frac{\xi\omega}{1-\omega^2}\right)\right)} = |F_{ts}^{(1)}| e^{j\varphi_{ts}^{(1)}} + f_d, \tag{4}$$

where θ_X^{ts} is the phase between the TSI force and the displacement which is governed by the force-distance relationship. If the contact is not conservative, θ_X^{ts} will slightly differ from 180° or 0°.

Equation (4) is a complex equation which can be solved for two unknowns by equating the real and imaginary parts of the two sides of the equality. All the results in this letter are calculated by solving Eq. (4) for the amplitude and phase of the TSI force using a gradient decent method.

The phase delay of the cantilever [$\arctan(\frac{\xi\omega}{1-\omega^2})$] also determines the sensitivity of the amplitude to the TSI force, which explains the relationship between the excitation frequency and the TSI force. Consider Fig. 5 which shows the phasor plot of the forces for two different excitation

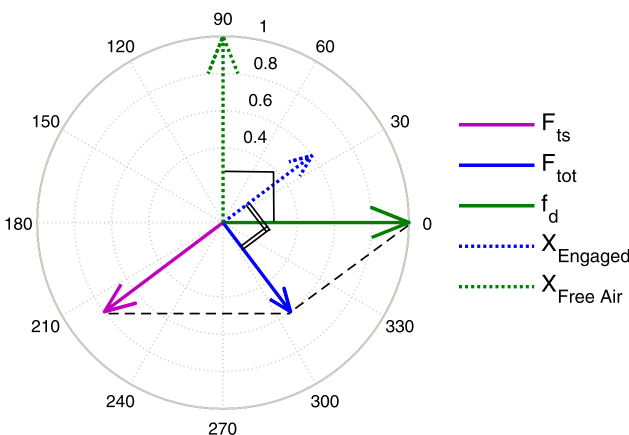

FIG. 4. Phasor plot of the forces and displacement in TM-AFM: The TSI force partially cancels the dither force, and hence, the amplitude reduces. Multimedia view: https://doi.org/10.1063/1.5016306.1

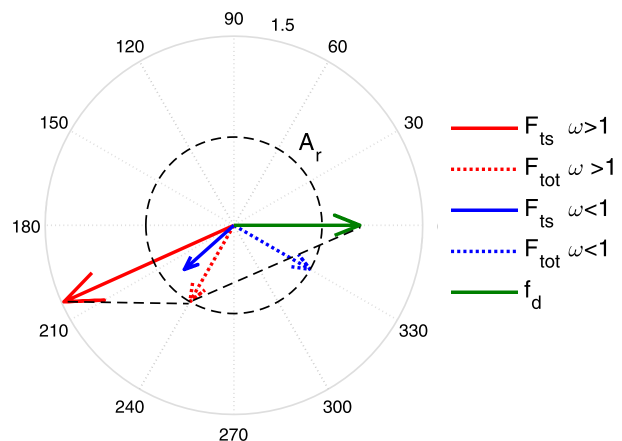

FIG. 5. Phasor plot of the forces in TM-AFM; Green: dither force, Blue: excitation frequency lower than resonance, and Red: excitation frequency higher than resonance frequency.

frequencies. To achieve a certain amplitude ratio, the amplitude of the total harmonic force should be A_r times the dither force, i.e., $F_{tot}^{(1)}$ should lie on the A_r circle in Fig. 5. As seen, there can be many different TSI forces, with different angles that can achieve this. Although the phase angle is determined by the displacement which itself depends on the total harmonic force and the linear dynamics of the cantilever, the TSI force should satisfy two conditions in a 2D space, a phase and an amplitude condition. Geometrically, the phase between the TSI force and the total harmonic force $[\theta_X^{ts} + \arctan(\frac{\xi\omega}{1-\omega^2})]$ determines the sensitivity of the cantilever to the TSI force. As seen, if this phase delay is closer to $0°$ $[\arctan(\frac{\xi\omega}{1-\omega^2})$ is closer to 180], then a higher TSI force is needed to reduce the total force and reach the A_r circle. In Fig. 5, both frequencies have equal dither force, free air amplitude, and amplitude ratio. However, for the red arrows, the excitation frequency is higher than the resonance frequency of the cantilever. Therefore, the phase delay of the cantilever $[\arctan(\frac{\xi\omega}{1-\omega^2})]$ is closer to $180°$, and consequently, a larger TSI force is required.

Figure 6 shows the magnitude of the first Fourier component of the force versus the amplitude ratio and the excitation frequency as obtained from Eq. (4). Note that in Figs. 6 and 2(a), the free air amplitude is constant and not the dither force. See supplementary material for more information on these trends. As it can be seen, the trends resemble the ones presented in Fig. 2(a). However, one should not compare the two graphs because Fig. 2(a) shows the PRF, while Fig. 6 shows the first Fourier component of the TSI force. In fact, Fig. 6 by its own cannot fully explain the nano-patterning experiments presented in Fig. 2(b) because the relationship between the damage/patterning and the first Fourier component of the TSI force is not known. Assuming a certain force model, one can estimate the PRF based on the first Fourier component of the TSI force, which might be more useful in estimating the damage. However, assuming a force model by itself can introduce large errors because many parameters and assumptions of the force models (e.g., tip-shape/size) are not measurable or verifiable in practice. To verify the results from the proposed formulation, we compare the first Fourier component of the force $[F_{ts}^{(1)}]$ calculated from Eq. (4) with that of the numerical solution of the fully nonlinear problem. See supplementary material for the details of the nonlinear model.

Figure 7 compares the forces achieved with the presented linear model and the numerical solution of the nonlinear model versus excitation frequency while keeping the amplitude ratio constant ($A_r = 0.7$). As shown in Fig. 7, the first Fourier component of the TSI force obtained by the linear model [Eq. (4)] agrees with the nonlinear model up to a numerical roundoff error (regardless of the parameters of the DMT model).

The presented model in Eq. (4) does not require the parameters of the force model, and it does not provide the PRF. However, at the frequency of interest (excitation and measurement frequencies), there is no difference between Eq. (4) and the fully nonlinear model. Hence, it can be concluded that the DMT modulus of the sample, i.e., surface elasticity, tip radius, Hamaker constant, etc., and the distance between the cantilever and the sample surface do not individually affect the amplitude and the phase of the cantilever at the frequency of interest. Consequently, they cannot be measured using conventional single frequency TM-AFM. This also explains why the height image of soft samples often depends on the imaging conditions and does not necessarily agree with their theoretical value.[13] The same reasoning holds for calculating the peak repulsive force or any other details of the TSI force. In general, since the amplitude and the phase of the first mode of the cantilever (the only observable signals) do not depend on the details of the tip-sample interaction force (DMT modulus, etc.), it is impossible to extract these details in TM-AFM without assuming a model for the force-distance relationship or performing a sweep measurement.

In conclusion, the origin of amplitude reduction in TM-AFM is explained by partial cancellation of the dithering force with the first harmonic component of the TSI force. The phase of the motion of the cantilever which is dominated by the excitation frequency governs the geometry of this interference. Therefore, the excitation frequency predominantly affects the TSI force. Moreover, only the first harmonic component of the TSI force participates in the working mechanism of the single-harmonic AFM. Hence, one cannot retrace

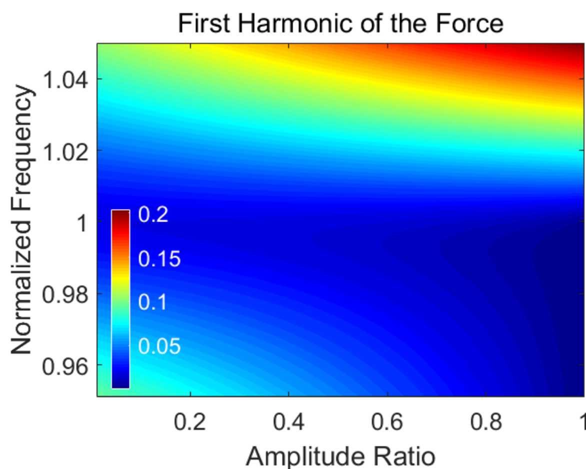

FIG. 6. Magnitude of the normalized first Fourier component of the tip-sample interaction force vs. amplitude ratio (horizontal) and excitation frequency (vertical).

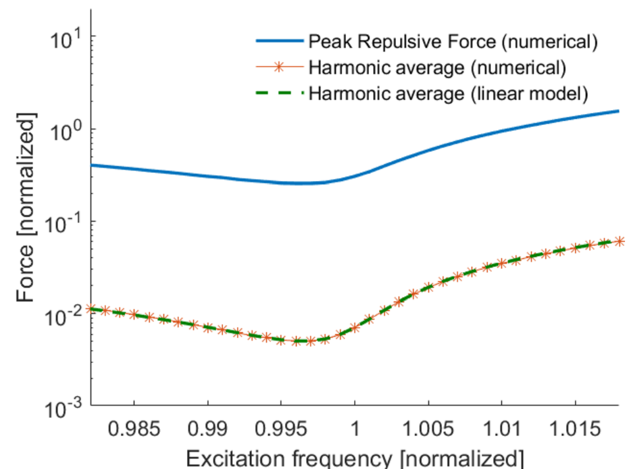

FIG. 7. Peak Repulsive Force and first Fourier component of the force vs. amplitude ratio ($A_r = 0.7$). The details of the full nonlinear mathematical model can be found in the supplementary material.

any information that is modulated on the higher harmonics of the TSI force. This is why the single-harmonic AFM does not even guarantee a correct measurement of the height profile, if the sample is not homogeneous.

See supplementary material for the details of the nonlinear model used for the comparison. The supplementary video shows the animated version of Fig. 4 for different amplitude ratios and different excitation frequencies.

This research was supported by Netherlands Organization for Applied scientific Research, TNO, Early Research Program 3D Nanomanufacturing.

[1]L. Wang, "Analytical descriptions of the tapping-mode atomic force microscopy response," Appl. Phys. Lett. **73**(25), 3781–3783 (1998).
[2]A. S. Paulo and R. Garcia, "Unifying theory of tapping-mode atomic-force microscopy," Phys. Rev. B **66**(4), 041406 (2002).
[3]S. I. Lee, S. W. Howell, A. Raman, and R. Reifenberger, "Nonlinear dynamic perspectives on dynamic force microscopy," Ultramicroscopy **97**(1), 185–198 (2003).
[4]S. Basak and A. Raman, "Dynamics of tapping mode atomic force microscopy in liquids: Theory and experiments," Appl. Phys. Lett. **91**(6), 064107 (2007).
[5]A. Keyvani, H. Sadeghian, H. Goosen, and F. van Keulen, "Transient tip-sample interactions in high-speed AFM imaging of 3D nano structures," Proc. SPIE **9424**, 94242Q (2015).
[6]R. Garcia and E. T. Herruzo, "The emergence of multifrequency force microscopy," Nat. Nanotechnol. **7**(4), 217–226 (2012).
[7]A. Keyvani, H. Sadeghian, M. S. Tamer, J. F. L. Goosen, and F. van Keulen, "Minimizing tip-sample forces and enhancing sensitivity in atomic force microscopy with dynamically compliant cantilevers," J. Appl. Phys. **121**(24), 244505 (2017).
[8]T. R. Rodriguez and R. Garcia, "Tip motion in amplitude modulation (tapping-mode) atomic-force microscopy: Comparison between continuous and point-mass models," Appl. Phys. Lett. **80**(9), 1646–1648 (2002).
[9]S. Hu and A. Raman, "Analytical formulas and scaling laws for peak interaction forces in dynamic atomic force microscopy," Appl. Phys. Lett. **91**(12), 123106 (2007).
[10]B. Xue, Y. Yan, Z. Hu, and X. Zhao, "Study on effects of scan parameters on the image quality and tip wear in AFM tapping mode," Scanning **36**(2), 263–269 (2014).
[11]C. Su, L. Huang, K. Kjoller, and K. Babcock, "Studies of tip wear processes in tapping mode atomic force microscopy," Ultramicroscopy **97**(1), 135–144 (2003).
[12]A. Keyvani, M. S. Tamer, M. H. van Es, and H. Sadeghian, "Simultaneous AFM nano-patterning and imaging for photomask repair," Proc. SPIE **9778**, 977818 (2016).
[13]A. L. Weisenhorn, M. Khorsandi, S. Kasas, V. Gotzos, and H.-J. Butt, "Deformation and height anomaly of soft surfaces studied with an afm," Nanotechnology **4**(2), 106 (1993).